A Computational Method for Determining Global Fuel−NO Rate Expressions. Part 1

ARTICLE *in* ENERGY & FUELS · SEPTEMBER 1996

Impact Factor: 2.79 · DOI: 10.1021/ef950169b

4 AUTHORS, INCLUDING:

Thomas H. Fletcher
Brigham Young University - Provo Main Cam…
155 PUBLICATIONS **2,289** CITATIONS
SEE PROFILE

Richard D. Boardman
Idaho National Laboratory
30 PUBLICATIONS **217** CITATIONS
SEE PROFILE

A Computational Method for Determining Global Fuel-NO Rate Expressions. Part 1

W. Chen,† L. D. Smoot,*,† T. H. Fletcher,† and R. D. Boardman‡

Chemical Engineering Department and Advanced Combustion Engineering Research Center, Brigham Young University, Provo, Utah

Received August 22, 1995⊗

Global chemical reaction rates used in the modeling of NO_x formation in comprehensive combustion codes have traditionally been obtained through correlation of experimental data. In this paper, a computational approach for obtaining global rates is presented. Several premixed flames were simulated, and sensitivity analysis of species concentration profiles was used to suggest global pathways in fuel-nitrogen conversion to NO. Based on these analyses, the global reaction rates were formulated. The predicted species concentration profiles and their derivatives were then used in the determination of the global rate constants. The correlation of rate constants for the two fuel-NO global rates ($HCN + NO \rightarrow N_2 + ...$ and $HCN + O_2 \rightarrow NO + ...$) are discussed. Comparisons of the computed global rate constants with those deduced from experimental data show good agreement. The global rates provide practical kinetics for simulating nitrogen pollutant chemistry in complex flames.

Introduction

Nitrogen oxides (NO_x) have been recognized as acid rain precursors that impose a significant threat to the environment. Coal combustion is a major anthropogenic source of NO_x. In coal combustion, NO_x originates mostly from nitrogen bound in the coal matrix, namely, fuel-NO_x.[1] Molecular nitrogen in air typically contributes less than 10% of the overall NO_x emissions from coal combustion.[2] Hence, this paper focuses on fuel-NO_x chemistry in hydrocarbon flames.

Detailed chemical kinetics of NO_x have been studied extensively and tabulated.[3,4] However, it is impractical to incorporate such elementary chemical kinetic schemes into a comprehensive combustion computer model with turbulent fluid dynamics, heat transfer, and chemical reactions because of unacceptable computer requirements. In addition, the formation and destruction rates of NO_x are of the same magnitude as turbulent mixing rates, and the equilibrium assumption is therefore not adequate in the calculation of NO_x concentrations.[5,6]

Several approaches have been developed and implemented to simplify the computation of chemical reactions of nitrogen species in hydrocarbon flames. Methods include the reduced reaction method, asymptotic method, sensitivity analysis method, partial equilibrium method, and multiconserved scalar method. In general, the implementation of these methods requires global or overall reaction schemes. These global schemes can be applied in the computation of NO_x concentrations in conjunction with turbulent fluid dynamics, heat transfer, and chemical reactions. Typically, only a few reaction steps and major species are considered in a global kinetic scheme instead of hundreds of reactions and species in a detailed reaction scheme. Consequently, computational time is also reduced significantly.

Traditionally, a global chemical kinetic pathway and associated rate constants have been obtained from correlation of experimental data. A limitation in correlating experimental data is that the range of reaction conditions may not have been broad enough to confidently apply the resulting global rates. It is also costly and sometimes very difficult to make the required measurements. A global sequence deduced from a large elementary step mechanism may include so many elementary rates and species concentrations that incorporation of those global reactions into comprehensive codes is still difficult. Although some elementary rates can be eliminated by additional assumptions, it is still difficult to apply such multireaction global schemes to comprehensive modeling, especially when turbulent combustion is encountered.[7]

This work was performed in order to deduce a global reaction rate for the reburning reaction $C_iH_j + NO \rightarrow HCN + ...$ Reburning has become a very important industrial process for the reduction of NO_x emissions during hydrocarbon fuel combustion. Being able to predict reburning phenomena can help substantially in

* Corresponding author address: Professor, Chemical Engineering, and Director, ACERC, 265L Crabtree Technology Building, Brigham Young University, Provo, Utah 84602. Phone: (801) 378−8930. Fax: (801) 378−6033.

† Advanced Combustion Engineering Research Center; Chemical Engineering.

‡ Adjunct Assistant Professor. Staff Engineer at Lockheed Martin Idaho Technologies, Idaho Falls, Idaho.

⊗ Abstract published in *Advance ACS Abstracts,* May 1, 1996.

(1) Smoot, L. D.; Boardman, R. D.; Brewster, B. S.; Hill, S. C.; Foli, A. K. Acid rain precursors model for practical furnaces. *Energy Fuels* **1993**, *7*, 786.

(2) Wendt, J. O. L. Fundamental coal combustion mechanisms and pollutant formation in furnaces. *Prog. Energy Combust. Sci.* **1980**, *6*, 1.

(3) Miller, J. A.; Bowman, C. Mechanism and modeling of nitrogen chemistry in combustion. *Prog. Energy Combust. Sci.* **1989**, *15*, 287.

(4) Peck, R. E.; Glarborg, P.; Johnsson, J. E. Kinetic modeling of fuel-nitrogen conversion in one-dimensional, pulverized coal flames. *Combust. Sci. Technol.* **1991**, *76*, 81.

(5) Bilger, R. W. Turbulent flow with nonpremixed reactants. In *Turbulent Reacting Flows*; ; Libby, P. A., Williams, F. A., Eds.; Topics in Applied Physics, Volume 44; Springer-Verlag: Berlin, Heidelberg, 1980.

(6) Drake, M. C.; Blint, R. J. Relative importance of nitric oxide formation mechanisms in laminar opposed-flow diffusion flames. *Combust. Flame* **1991**, *83*, 185.

(7) Smooke, M. D. *Lecture notes in physics: Reduced kinetic mechanisms and asymptotic approximations for methane-air flames*; Springer-Verlag; Berlin, 1991; Vol. 384.

S0887-0624(95)00169-1 CCC: $12.00

the design and optimization of such systems. Yet no global reaction rate suitable for inclusion in a comprehensive combustion code has ever been reported. In this Part 1 paper, a method for obtaining a global chemical reaction rate expression and its associated rate constant is presented and the correlations from this method are compared with the correlations based on experimental data.[8] By use of a comprehensive set of elementary chemical reactions steps, a series of simulations of premixed flames was made and sensitivity analysis of the predicted nitrogen species in these flames was completed. Based on the simulations and sensitivity analysis, global reaction pathways are suggested and the global rate expressions are formulated. Furthermore, the global reaction rates in these rate expressions are correlated from species concentration profiles obtained from the full mechanism simulations. In a companion paper, this method is applied to the determination of the rate of a NO_x global reburning reaction. [9]

Computational Method

Approach. Premixed flames were simulated with elementary chemical kinetics in order to (1) demonstrate the capability of simulating the reacting process, (2) provide complete species profiles with respect to time for use in the development of global rate expressions, and (3) conduct sensitivity analyses based on the predicted species profiles, to be used to help identify the rate-determining reactions. Comparisons of predicted and measured premixed flame species and temperature have been previously reported by several researchers (e.g., refs 3, 4, and 10). The comparisons of species concentration profiles establish the accuracy of the local species concentration predictions, which are used in subsequent global reaction rate correlations.

A reaction scheme with 254 gaseous elementary reactions was used in the simulations of NO formation in premixed, laminar hydrocarbon-containing flames, together with the CHEMKIN code.[11] Of these 254 steps, 234 reactions are from Miller and Bowman[3] (1989), and the balance are from Tables 2 and 3 in Zabarnick,[12] which add more NO_2 and N_2O steps to the Miller and Bowman scheme. Rate constants used for this study were those reported by Zabarnick et al.,[13] Miller and Bowman,[3] and Zabarnick.[12]

Rate-determining steps of the NO formation process were identified by using the SENKIN program,[11] which calculated the sensitivity coefficients

$$S_{ij} = \frac{\partial C_i}{\partial k_j} \tag{1}$$

where C_i is the concentration of species i, k_j is the rate constant of the reaction j, and S_{ij} is the sensitivity coefficient of species i with respect to the reaction j based on the rate constant k_j.

The elementary chemical reactions used in this study are assumed to be sufficient and appropriate for the simulations of hydrocarbon combustion and NO formation. The application of the reaction set to different premixed flames is also assumed to be appropriate. The comparisons of experimental data and calculations help to verify these assumptions.

Temperature Profiles. Measured temperature profiles were used for the simulations rather than those from solution of the energy equation. Temperature profiles for the cases that only reported effluent temperatures were determined by the method Gardiner,[14] based on other available temperature profiles in the same reactor and burner configuration, as follows:

$$\frac{T_2}{T_1} = \left(\frac{X_2}{X_1}\right)^R \tag{2}$$

where X_1 and T_1 are the mole fraction of the limiting reactant and temperature at the known condition, and X_2 and T_2 are the mole fraction and temperature at the corrected conditions. The index R varies from 1.58 to 3.42 as a function of equivalence ratio.[8] Ambient temperature was assumed to be the initial temperature, and a linear temperature profile was assumed between the ambient temperature and the experimental starting temperature. The agreement of the measured rate constants with computed values based on the corrected temperature profiles validated this temperature correction method, although accurate temperature measurements may have further improved the predictions of species profiles.

Rate-Determining Reactions. Depending on combustion conditions, some steps in a large set of reactions may be more significant than others to nitrogen pollutant formation processes. The overall formation and destruction rate of NO_x will depend on these rate-determining reactions. However, because rates are determined by the concentrations of products and reactants and temperature, the rate-determining reactions may change as concentrations and temperatures vary. Therefore, it is important to use the full set of available elementary chemical kinetic rates when seeking to identify a global rate that incorporates the dependence of the rate-controlling steps over a wide range of conditions. The rate-determining reactions are not always known when an empirically derived global mechanism is obtained. Even when the rate-determining reactions are known, the lack of experimental data over a broad range of conditions may limit the applicability of the empirically derived rate constants. However, through the use of a detailed reaction set, the variation of rate-determining reactions can be readily determined.

Time Scales. Hydrocarbon reactions and radical reactions are usually referred to as fast reactions, while most nitrogen reactions are comparatively slow.[15] Therefore, in the calculation of complex, turbulent diffusion flames, hydrocarbon reactions and O_2-H_2 reactions are

(8) Chen, W. A global rate of nitric oxide reburning. Ph.D. Dissertation, Department of Chemical Engineering, Brigham Young University, Provo, Utah, 1994.

(9) Chen, W.; Smoot L. D.; Hill, S. C.; Fletcher, T. H. A global rate expression for nitric oxide reburning. Part 2. *Energy Fuels* **1996**, *10*, 1046.

(10) Kramlich, J. C.; Cole, J. A.; McCarthy, J. M.; Lanier, W. S. Mechanisms of nitrous oxide formation in coal flames. *Combust.Flame* **1989**, *77*, 375.

(11) Kee, R. J.; Rupley, F. M.; Miller, J. A. Chemkin-II: A FORTRAN chemical kinetics package for the analysis of gas-phase chemical kinetics. SAND89−8009.UC-401, Sandia National Laboratories: Albuquerque, NM, 1991.

(12) Zabarnick, S. A comparison of $CH_4/NO/O_2$ and CH_4/N_2O flames by LIF diagnostics and chemical kinetic modeling. *Combust. Sci. Technol.* **1992**, *83*, 115.

(13) Zabarnick, S.; Fleming, J. W.; Lin, M. C. Kinetics of CH radical reactions with propane, isobutane and neopentane. *Chem. Phys.* **1987**, *112*, 409.

(14) Gardiner, W. C., Jr. *Combustion Chemistry*; Springer-Verlag: New York, 1984.

(15) Bilger, R. W. Reaction rate in diffusion flames. *Combust. Flame* **1978**, *30*, 277.

Table 1. Experimental Data of Premixed Flames for Simulation

no.	author(s)	fuel and oxidizer	fuel-nitrogen	comments
1	De Soete[19−21]	fuel: C_2H_4 and CH_4 oxidizer: oxygen and air	C_2N_2, NO, N_2, ammonia	79 cases are available. N_2 is added into hydrocarbon flames to study the prompt-NO exclusively.
2	Thompson et al.[22]	fuel: CH_4 oxidizer: air	no fuel-N	Six cases are available. Cases are for thermal and prompt-NO studies.
3	Morley[23]	fuel: CH_4, C_2H_2, C_2H_4, acetylene oxidizer: air, oxygen−nitrogen	NH_3, NO, CH_3CN, pyridine	Sixteen cases are available. HCN, NO, NH_3, and H_2CN^+ profiles are plotted, and three mechanisms are proposed to evaluate the kinetic pathways of HCN oxidation.
4	Haynes,[24,25] Haynes et al.[26]	fuel: CH_4, C_2H_2, C_2H_4 oxidizer: air, O_2-N_2	pyridine, C_2N_2, NH_3	21 cases are available. Behavior of nitrogen components and radicals in fuel-rich flames was studied.
5	Hayhurst and Vince[27]	fuel: CH_4, C_2H_6, C_2H_4, C_2H_2, C_6H_6, CH_3OH oxidizer: air, O_2-N_2, O_2	NH_3, NO, pyridine, HCN, N_2O, their mixtures	More than 153 cases are available. Study focuses on the role of prompt-NO, and HCN formation and destruction.

often considered to be in equilibrium.[5,15,16] In diffusion flames, the mass transport time scale is much larger than the reaction time scale for hydrocarbon reactions and O_2-H_2 reactions.[16,17] Therefore, for many turbulent combustion problems, local hydrocarbon and O_2 reactions can be calculated by the transport equation assuming instantaneous equilibrium.

The equilibrium assumption is not adequate for simulations of premixed flames. In laminar, premixed flames, an inlet stream carries mixed fuel and oxidizer into the reaction zone, and products along with any unreacted reactant and oxidizer travel downstream. Generation and consumption of intermediates and radicals occur in a narrow flame zone. These radicals and intermediates may act as the initiators or reactants in the relatively slow nitrogen reactions. For example, the reburning-NO process, referring to the reduction of nitrogen oxides to HCN and finally to N_2 by hydrocarbons (i.e., HC + NO → HCN + ... $\xrightarrow{NO}$ N_2 + ...) is part of the complete NO reaction sequence.[18] In the reburning-NO mechanism, the rates of elementary HCN formation reactions are of the same magnitude as those of hydrocarbon reactions. Therefore, reburning-NO reactions could be considered as the connection between the fast hydrocarbon reactions and slow nitrogen reactions.

The equivalence ratio in a diffusion flame typically varies continuously from the most fuel-rich at the primary inlet to the most fuel-lean at the secondary inlet. Therefore, the importance of the reburning-NO mechanism in such flames is expected to change locally. Alternatively, premixed flame simulations with different equivalence ratios can be considered as simulations of diffusion flames at various locations in the reactor. The approach used herein has been to derive global rate expressions from laminar premixed flames with the expectation that such global rates can be used in the simulation of nitrogen reactions in turbulent diffusion flames.

Simulations and Sensitivity Analysis

Premixed, laminar flames were simulated with CHEMKIN[11] and the comprehensive reaction scheme referenced above in order to (1) provide insight into flame characteristics, (2) provide a basis for evaluation of the kinetic mechanisms through comparison with measured flame species profiles, (3) provide computed results for sensitivity analysis to help identify controlling reactions and subsequently global reaction schemes, and (4) provide computed species profiles for correlating rate parameters for the postulated global reactions. Several flames were simulated to provide insight over a range of flame conditions. Since a premixed flame occupies a very thin region spatially, it is easier to display such flames on a time-resolved basis in order to stretch the thin flame into a wider domain.

Experimental Cases. Selection of experimental data for simulation requires the availability of measured temperature profiles and initial species concentrations. Several sets of experimental data for premixed flames (noted in Table 1) were identified for simulation and data comparison. Complete illustrations of all simulations and comparisons for the cases in Table 1 are given by Chen,[8] with some cases presented herein. Time-resolved species profiles were calculated for evaluation and comparison with the experimental measurements.

De Soete[19−21] conducted extensive experiments on the formation of nitrogen-containing pollutant species in premixed flames. From a correlation of these experimental results, a set of global reactions and corresponding rate constants were determined. Both temperature profiles and input parameters, as well as species profiles (especially nitrogen species), are reported for De Soete's experiments. Methane (CH_4) and ethylene (C_2H_4) were used as fuels, with NO, C_2N_2, or ammonia (NH_3) being added as fuel-nitrogen sources. Although this work was performed over two decades ago, global rates of NO formation from fuel-nitrogen measured in those studies are still widely used in predictions of fuel-NO_x in

(16) Drake, M. C.; Pitz, R. W.; Lapp, M.; Fenimore, C. P.; Lucht, R. P; Sweeney, D. W.; Laurendeau, N. M. Measurements of superequilibrium hydroxyl concentrations in turbulent nonpremixed flames using saturated fluorescence. *Twentieth Symposium (International) on Combustion*; The Combustion Institute: Pittsburgh, PA, 1984; p 327.

(17) Libby, P. A.; Williams, F. A. *Turbulent Reacting Flows*; Topics in Applied Physics, Vol. 44; Springer-Verlag: Berlin, Heidelberg, 1980.

(18) Wendt, J. O. L.; Bose, A. C.; Hein, K. R. G. Fuel nitrogen mechanisms governing NO_x abatement for low and high rank coals. Joint Symposium on Stationary Combustion NO_x Control, San Francisco, CA, 1989.

(19) De Soete, G. C. Nitric oxides' formation and decomposition in the combustion of hydrocarbon flames (La Formation et la Decomposition d'Oxyde Nitrique dans les Produits de Combustion de Flammes d'Hydrocarbures). *Rev. Pet. Inst. France* **1972**, *xxvii*, 372.

(20) De Soete, G. C. Mechanisms of nitric oxides from ammonia and amines in hydrocarbon flames (Le Mechanisme de Formation d'Oxyde Azotique A Partir D'Ammoniac et d'Amines dans les Flammes d'Hydrocarbures). *Rev. Pet. Inst. France* **1973**, *xxviii*, 171.

(21) De Soete, G. C. Overall reaction rates of NO and N_2 formation from fuel nitrogen. *Fifteenth Symposium (International) on Combustion*; The Combustion Institute: Pittsburgh, PA, 1975; p 1093.

combusting hydrocarbon−air systems. These rates are thus given special consideration in this work.

Thompson et al.[22] measured NO concentrations in premixed methane−air flames without the addition of the fuel-N source. In their measurements, part of the NO (70%) was formed very early in the flames. This may have been caused by prompt-NO reactions. The remainder of the NO (30%) was formed gradually along the tubular reactor, presumably by thermal-NO reactions. In the center of the tubular reactor, the NO concentration was observed to be higher than near the wall. This also was attributed to the thermal-NO mechanism, since thermal-NO reactions are slow and depend on the reaction temperature. Therefore, the data provided by these experiments were selected as a basis to simulate joint formation of thermal-NO and prompt-NO reactions. Comparisons of HCN from the prompt-NO steps, in which HCN is formed only from molecular nitrogen, with the reburning-NO steps, in which HCN is formed through NO reduction, can help in understanding the significance of the reburning-NO reactions.

Morley[23] added different fuel-nitrogen compounds to hydrocarbon flames to study the interactions between fuel-nitrogen and hydrocarbons. He found that the formation of HCN was directly proportional to the reduction of NO in fuel-rich flames. Simulation of this flame provides insight to HCN oxidation pathways.

Simulations of the flames of Haynes[24,25] and Haynes et al.[26] show an increase in HCN concentration with increased NO seeding in $C_2H_4-O_2-N_2$ flames. In Haynes' experiments, NO reduction is proportional to the concentration of NO seeding in the flames. The reduction of NO indicates the significance of the reburning-NO reactions. Premixed flames with different equivalence ratios and different feed NO concentrations are used to approximate various locations in a diffusion flame. Therefore, the significance of reburning-NO reactions in diffusion flames can be inferred from these premixed data.

Hayhurst and Vince[27] compiled data for several hydrocarbon flames that included the interactions between hydrocarbons and NO. They also studied the role of NH_i (i = 1, 2, and 3) in fuel-rich flames, concluding that NH_i is less significant than HCN in environments rich in hydrocarbon radicals. Similar premixed flames have been investigated by other investigators. [28]

Simulations with Elementary Kinetics. Simulations for many of the premixed flames listed in Table 1 were made to deduce the global mechanisms after the rate-determining reactions were identified by performing a sensitivity analysis and through previous published work.[19−21]

The characteristics of NO profiles in fuel-lean flames and in fuel-rich flames can be deduced from these simulations. The effects of different fuel-N species on the NO concentration profiles were determined. Comparisons of NO profiles with and without NO seeded into the flames provided evidence of the significance of the reburning-NO mechanism.

Measured temperature profiles from De Soete[21] were correlated with a third-order polynomial to within 3% for subsequent use in this analysis. Figure 1 presents a series of simulations of the $C_2H_4-O_2$ flames with the equivalence ratio (ϕ) varying from 0.75 to 1.53. In these simulations, the initial concentration of fuel-N, which is C_2N_2, was kept constant (C_2N_2 = 260 ppm). Argon was used as the carrier gas rather than N_2 to eliminate the thermal-NO effect.

The predicted conversion of fuel-N to NO varies with ϕ, achieving a peak of 253 ppm at $\phi = 1.0$ and dropping to 130 ppm at $\phi = 1.53$. This observation is consistent with the findings of previous investigators.[23,29,30] Under fuel-lean conditions ($\phi < 1.0$), NO profiles have three distinct regions (parts a and b of Figure 1). In the early flame, because of low HCN concentrations, the NO formation rate is relatively low. Within the flame, which is a very narrow region, the concentrations of radicals such as O, OH, and CH_i are relatively high and combustion proceeds quickly. The high radical concentrations accelerate the transformation of nitrogen species to NO. Hence, NO has a very high formation rate. After the flame region, a slow NO formation region exists where radical concentrations are very low. If high temperature is maintained, the excess O_2 is dissociated further and reacts with N_2 to form NO through the thermal-NO mechanism.

When the flames are somewhat fuel-rich (Figure 1d), there are four distinct regions for NO formation. The first and third regions have higher formation rates because of radical-rich conditions. A plateau between the first and third periods is a period of slow formation rate. This may be caused by the fact that the NO concentration in this region is so high that the reburning NO mechanism becomes significant. In this region, partial equilibrium between NO and HCN exists until the completion of combustion. With the completion of combustion, the radical-rich pool disappears and the relatively high concentration of HCN cannot be sustained. The postflame region in slightly fuel-rich flames is similar to the fuel-lean region because of the lack of the radicals.

Under very fuel-rich conditions (parts e and f of Figure 1), NO formation is relatively slow in the first region compared to fuel-lean flames. The absence of oxidizing species results in a low NO formation rate, even though HCN concentrations are relatively high. When NO achieves a certain level, the reactions between hydrocarbon radicals and NO yield a significant concentration of HCN after the first region. In this postflame region, hydrocarbon radicals cannot be oxidized completely and NO reduction by hydrocarbon radicals

(22) Thompson, D.; Brown, T. D.; Beer, J. M. NO_x formation in combustion. *Combust. Flame* **1972**, *19*, 69.
(23) Morley, C. The formation and destruction of hydrogen cyanide from atmospheric and fuel nitrogen in rich atmospheric-pressure flames. *Combust. Flame* **1976**, *27*, 189.
(24) Haynes, B. S. Reactions of ammonia and nitric oxide in the burnt gases of fuel-rich hydrocarbon-air flames. *Combust. Flame* **1977**, *28*, 81.
(25) Haynes, B. S. The oxidation of hydrogen cyanide in fuel-rich flames. *Combust. Flame* **1977**, *28*, 113.
(26) Haynes, B. S.; Iverach, D.; Kirov, N. Y. The behavior of nitrogen species in fuel-rich hydrocarbon flames. *Fourteenth Symposium (International) on Combustion*; The Combustion Institute: Pittsburgh, PA, 1973; p 1103.
(27) Hayhurst, A. N.; Vince, I. M. Nitric oxide formation from N_2 in flames: The importance of 'prompt' NO. *Prog. Energy Combust. Sci.* **1980**, *6*, 35.
(28) Lisa, D. P.; Stuart, W. C. Effect of fuel sulfur on nitrogen oxide formation in a thermally stabilized plug-flow burner. *Ind. Eng. Chem. Res.* **1989**, *28*, 1104.
(29) Fenimore, C. P. Formation of nitric oxide from fuel nitrogen in ethylene flames. *Combust. Flame* **1972**, *19*, 289.
(30) Fenimore, C. P. Studies of fuel-nitrogen species in rich flame gases. *Seventeenth Symposium (International) on Combustion*; The Combustion Institute: Pittsburgh, PA, 1979; p 661.

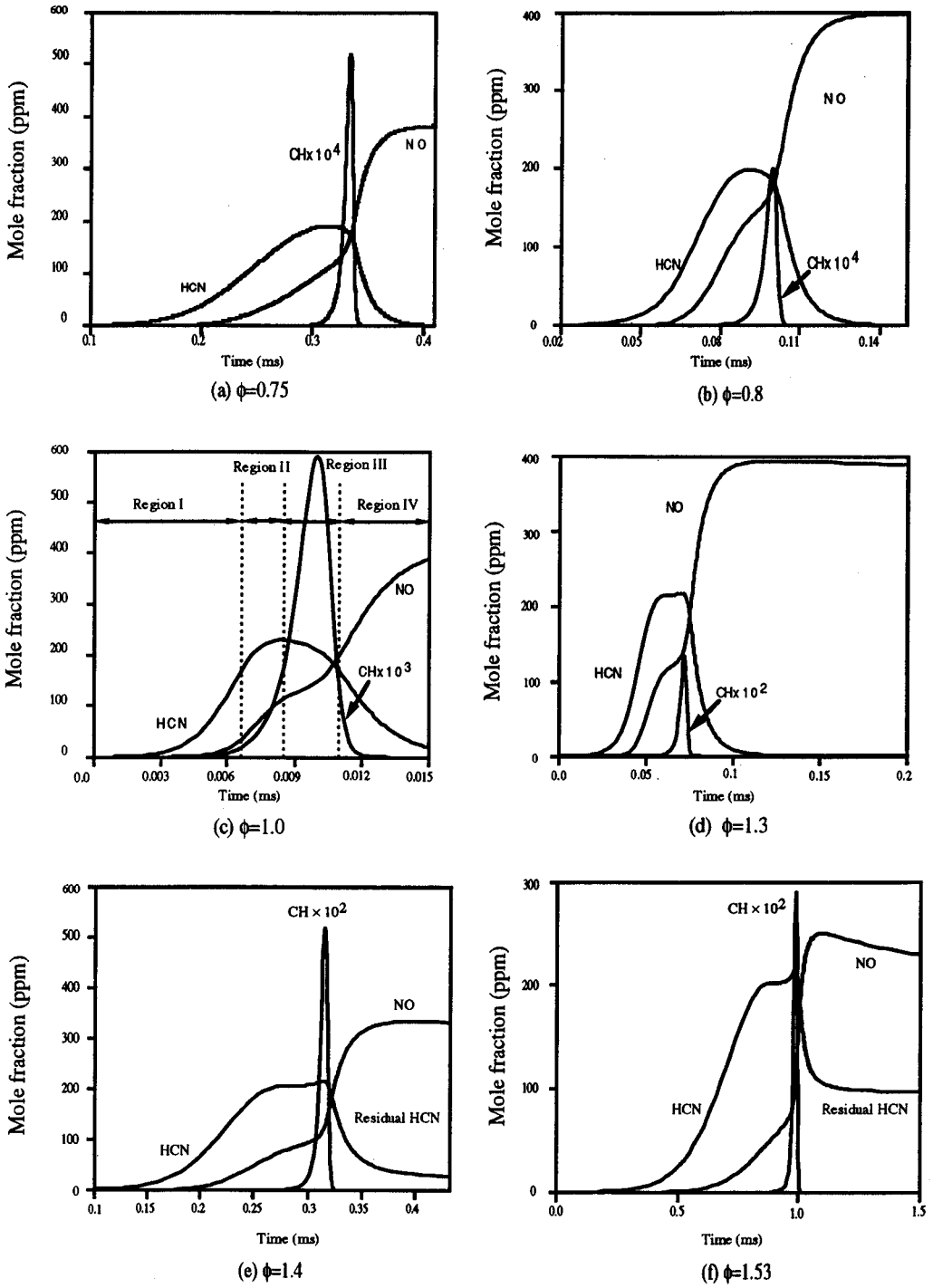

Figure 1. Predicted species concentration profiles of $C_2H_4-O_2-Ar$ flames with C_2N_2 (260 ppm) as fuel-N. Flame conditions are the same as those of De Soete.[21]

becomes dominant. HCN continues to form NO and N_2, and this cycle depletes NO until a partial equilibrium state is reached.

The effect of fuel-N on the reduction of NO can be seen in Figure 2. NO concentration reaches a maximum at $\phi = 1$ for different concentrations of fuel-N. The high equivalence ratio results in low NO production because of the reburning process. In general, the amount of NO reduced is increased when more fuel-N exists. However, the ratio of NO reduced to the peak NO is not changed substantially. When NO is added directly to the flame, the NO concentration is reduced by the reburning-NO mechanisms and a significant amount of HCN is formed (in Figure 3). The similar slopes of the HCN and NO profiles imply that HCN is formed at the same rate that NO is reduced. The sum of the NO and HCN concentrations in the postflame region is approximately equal to the initial NO concentration, further implying that most of the NO reduced through the reburning-NO mechanism is transformed to HCN.

HCN is an important intermediate between fuel-N and NO. The fate of HCN determines the amount of NO in the exhaust gases. In fuel-lean to slightly fuel-rich flames, HCN reaches a peak and then is completely depleted (as shown in Figure 1). At this location where HCN begins to decrease, NO is formed quickly and NO reaches a maximum when the HCN is completely consumed. In very fuel-rich flames, HCN cannot be

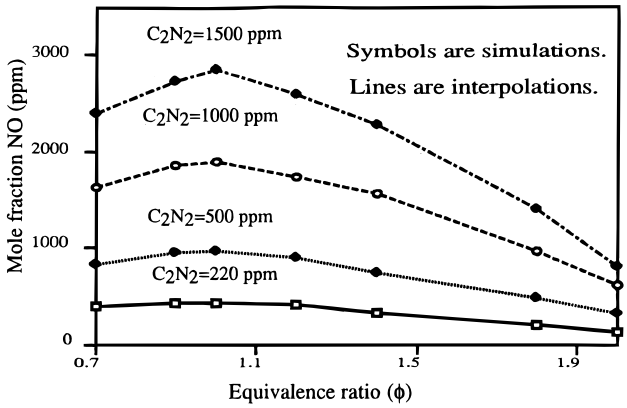

Figure 2. Simulations showing dependence of NO on equivalence ratio (ϕ) for $C_2H_4-Ar-O_2-C_2N_2$ flames, with Ar = 0.676. Input conditions are the same as those for the flames of De Soete.[21]

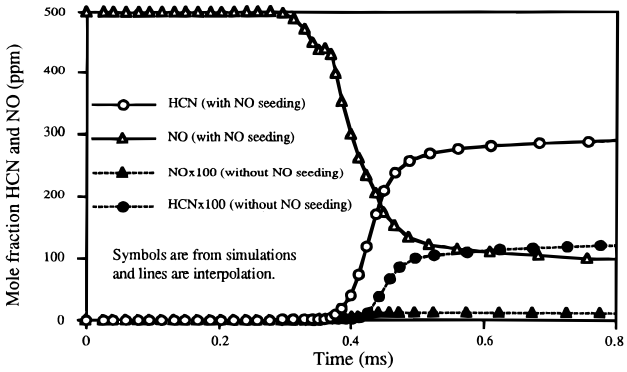

Figure 3. Predicted HCN formation with and without NO seeding for $C_2H_4-N_2-O_2$ flames and $\phi = 1.84$. NO (seeded) = 500 ppm. Flame conditions are the same as those from Haynes.[25]

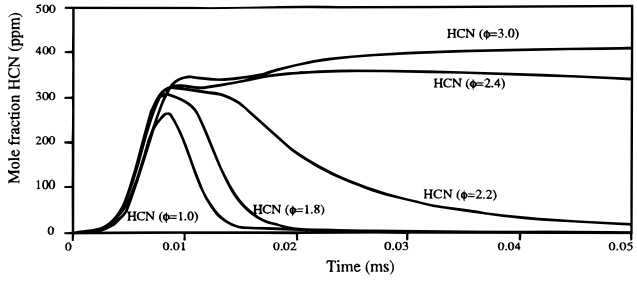

Figure 4. Predicted effects of equivalence ratio on HCN formation for $C_2H_4-Ar-O_2$ flames. C_2N_2 = 265 ppm. Flame conditions are the same as those from De Soete.[21]

consumed completely in the postflame regions, and partial equilibrium between HCN and NO may exist because of the reburning-NO mechanism. There may also be a significant amount of HCN remaining, which is called residual HCN (see Figures 1 and 4).

Under some fuel-rich conditions, the amount of residual HCN remains nearly constant, while the NO concentration is slightly reduced (Figure 1f). Although the HCN concentration appears to be unchanged, NO reburning may still be occurring, with HCN being converted to N_2, because NO concentration continues to decrease.

When NO seeding is used in a fuel-rich hydrocarbon flame (Figure 4), the HCN profile is different from the HCN profiles exhibited by fuel-rich flames with fuel-N additives. No peak in NO concentration is observed. Rather, the HCN concentration is almost constant after

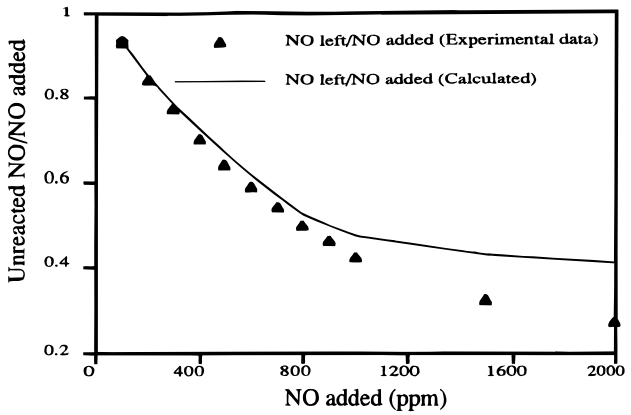

Figure 5. NO remaining from fuel-rich hydrocarbon flames (ethylene–argon flames). $\phi = 2.05$, and $T = 2530$ K. Flame conditions are the same as those from Morley.[23]

the flame zone (Figure 3). However, the NO concentration continues to decrease while HCN remains constant. The relationship between NO and HCN in this case is similar to the zone where residual HCN exists in fuel-rich flames (Figure 1d). In other words, NO is constantly reduced through the reburning-NO mechanism that forms HCN. In addition, HCN cycles to NO with a certain amount being reduced to N_2.

HCN can also be formed through the prompt-NO mechanism when hydrocarbon radical concentrations are high. In Figure 5, comparisons of predicted and experimental NO reduction show that a significant amount of NO is reduced under the conditions simulated ($\phi = 2.05$). The simulations and comparisons without fuel-N show that the amount of HCN (<3 ppm) formed throughout the prompt-NO mechanism is much less than the HCN (>440 ppm) formed from the fuel-N mechanism (Figure 1) and from the reburning-NO steps (HCN > 280 ppm in Figure 3). Prompt-NO is generally negligible when a certain amount of fuel-NO exists.

In summary, fuel-N conversion to NO is lower in fuel-rich flames than in stoichiometric flames. When hydrocarbon flames are seeded with NO, the NO concentrations are substantially reduced and high HCN concentrations are observed. The NO reduction to HCN can be attributed to the reburning-NO mechanism. However, further sensitivity analysis is needed to identify whether the reburning-NO steps are significant in these flames.

NH_3 addition to gaseous hydrocarbon flames has been examined by De Soete,[20] Haynes et al.,[26] Hayhurst and Vince,[27] and Miller and Bowman.[3] NH_3 has also been observed as an important fuel-N species released from coal particles.[13,18,31,32] Generally, the elementary reactions of NH_3 are relatively fast, and NH_3 decomposition at high temperatures involves many elementary steps.[33,34]

(31) Wendt, J. O. L.; Sternling, C. V.; Matovich, M. A. Reduction of sulfur trioxide and nitrogen oxides by secondary fuel injection. *Fourteenth Symposium (International) on Combustion*; The Combustion Institute: Pittsburgh, PA, 1973; p 897.

(32) Bassilakis, R.; Zhao, Y.; Solomon, P. R.; Serio, M. A. Sulfur and Nitrogen Evolution in the Argonne Coals: Experiment and Modeling. *Energy Fuels* **1993**, *7*, 710.

(33) Westenburg, A. A.; DeHaas, N. Atom-molecule kinetics using USR detection. *J. Chem. Phys.* **1969**, *10*, 5215.

(34) Meienburg, W; Neckel, H.; Wolfrum, J. In situ measurement of ammonia with a $^{13}CO_2$-waveguide laser system. *J. Appl.Phys. B* **1990**, *5*, 2, 94.

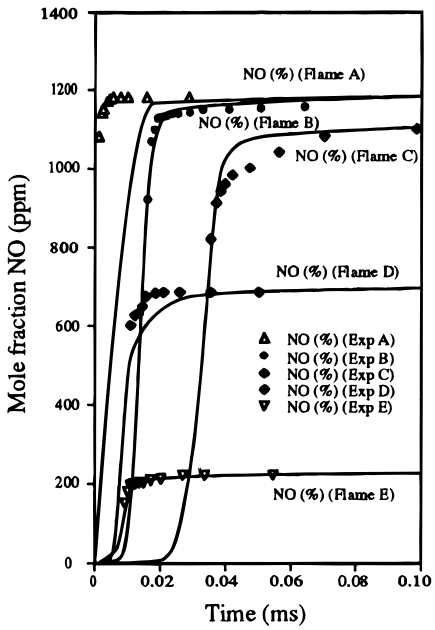

Flame A: NH_3 = 1490 ppm
Flame B: NH_3 = 1400 ppm
Flame C: NH_3 = 1330 ppm
Flame D: NH_3 = 790 ppm
Flame E: NH_3 = 250 ppm

Figure 6. NO profile comparisons between elementary simulations and experimental measurements (data from De Soete[20]). (Fuel = 7.2% C_2H_4; fuel-N = NH_3; O_2 = 21.7%; He = 70.9%.)

Two purposes in the simulations of NH_3 as fuel-N are (1) to determine whether the reburning-NO mechanism is significant in these flames and (2) to compare the measured reaction rates by De Soete[21] with those deduced from the simulations. The C_2H_4 and O_2 concentrations in these data are near stoichiometric. Therefore, the conversion of NH_3 to NO is expected to be high.[35] Polynomial correlations[21] used in the computation are within 2% of the measured temperatures. Helium (70.9%) was used as the carrier gas to eliminate thermal-NO and prompt-NO effects.

The simulations illustrated in Figure 6 show high NO production in $C_2H_4-NH_3-O_2-He$ flames. The high NO yield implies that the reburning-NO mechanism is insignificant under these combustion conditions, since the reburning-NO mechanism would have otherwise substantially reduced the NO concentration. In Figure 7, the effluent NO from $C_2H_4-NH_3-O_2-He$ flames is illustrated. Under fuel-rich conditions, NH_3 flames exhibit the same trend as the C_2N_2-seeded flames, where the reburning-NO mechanism does appear to be important.

Comparisons between simulations and experimental data are shown in Figures 5−7. The simulations for stoichiometric flames usually give the best agreement with the experimental data. The simulations disagree more with the data in the extreme fuel-rich and fuel-lean regions. The disagreement may be caused by the incompleteness of the elementary kinetic steps and rates, errors from extrapolating the temperature profiles, or inaccuracy of the measurements. Consequently, limitations in the comprehensive reaction mechanism may result in inaccuracies in the global rates subsequently deduced from this mechanism.

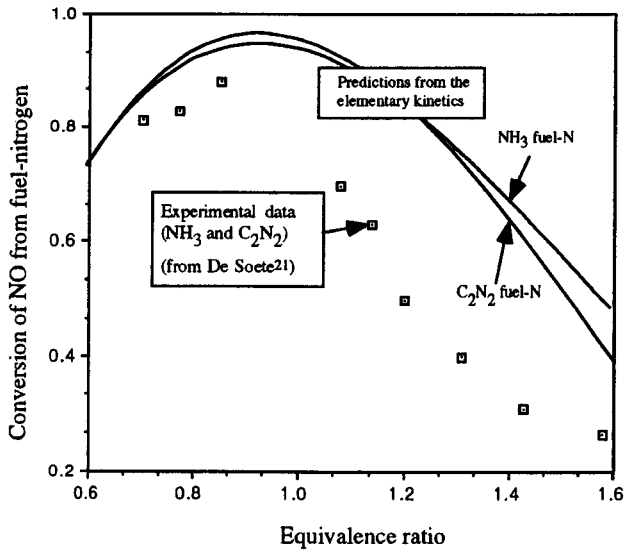

Figure 7. Comparisons of predicted fuel-nitrogen conversion from elementary chemical kinetics with experimental data from De Soete.[21]

Global Fuel-NO Rate Expressions

Global Fuel-NO Pathway. In the simulations reported above, C_2N_2 and NH_3 were used as fuel-N. HCN is observed very early in the flame, and its oxidation leads to the formation of NO in the flames with C_2N_2 as fuel-N. HCN is an intermediate between fuel-N and NO and connects the fuel-NO and reburning-NO steps. Therefore, the following global reaction from fuel-N to HCN can be assumed:

$$\text{fuel-N} \rightarrow \text{HCN} \qquad (3)$$

HCN formed from fuel-N can be further oxidized to NO or N_2.[3,10,21,36] The oxidation pathway of HCN includes the following mechanistic steps:

$$\text{HCN} + \text{O} \rightarrow \text{NCO} + \text{H} \qquad (4)$$

and

$$\text{NCO} + \text{O} \rightarrow \text{NO} + \text{CO} \qquad (5)$$

or

$$\text{NCO} + \text{H} \rightarrow \text{NH} + \text{CO} \qquad (6)$$

and then

$$\text{NH} + \text{O} \rightarrow \text{NO} + \text{H} \qquad (7)$$

The above steps (i.e., 4−7) can be combined algebraically with $H + H + M \rightarrow H_2 + M$, $H_2 + O \rightarrow OH + H$, and $OH + H + M \rightarrow H_2O + M$ to yield the global reaction

$$\text{HCN} + \text{O}_2 \rightarrow \text{NO} + \ldots \qquad (8)$$

HCN can also form NCO, HCNO, and NH_i radicals by

(35) Duo, W.; Dam-Johansen, K.; Ostergaard, K. Kinetics of the gas-phase reaction between nitric oxide, ammonia and oxygen. *Can. J.Chem. Eng.* **1992**, *70*, 1014.

(36) Bose, A. C.; Dannecker, K. M.; Wendt, J. O. L. Coal combustion effects on mechanisms governing the destruction of NO and other nitrogenous species during fuel-rich combustion. *Energy Fuels* **1988**, *2*, 301.

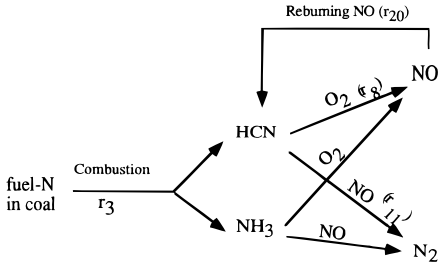

Figure 8. Global fuel-N to NO pathway.

the following reactions:

$$HCN + O \rightarrow NCO + N + ... \rightarrow N_2 + CO + ... \quad (9)$$

and

$$HCN + H \rightarrow NH + N + ... \rightarrow N_2 + H + ... \quad (10)$$

Similar to the global HCN oxidation pathway (eq 8), the global HCN reduction pathway can be written as follows by algebraic combination of fundamental reactions:

$$HCN + NO \rightarrow N_2 + ... \quad (11)$$

The rate constants of global reactions 8 and 11 were obtained by De Soete[21] by correlating laboratory data. A comparison of the correlations deduced from the simulations herein with the laboratory data correlations by De Soete[21] is given subsequently.

Differential Rate Equations. From the simulations, the two characteristic times, where $dX_{HCN}/dt = 0$, are defined as t_1 and t_2 (Figure 1). The quantity t_1 characterizes the maximum concentration of HCN. The quantity t_2 occurs at long residence times after the variation of HCN with respect to time becomes zero because of relatively low hydrocarbon radical concentrations (CH_i). These two characteristic times always exist from fuel-lean to fuel-rich (Figure 1). Whether or not the reburning-NO mechanisms is significant, t_1 and t_2 are observed.

For fuel-lean flames, the reburning-NO process can be neglected. Figure 8 shows the global reaction sequence being considered, which includes HCN and NH_3 reaction processes. By material balance, referring to Figure 8, the depletion rate of nitrogen atoms by the global reactions 8 and 11 was expressed by De Soete[21] as follows:

$$-\frac{dX_{HCN}}{dt} = 2\frac{dX_{N_2}}{dt} + \frac{dX_{NO}}{dt}, \quad t > t_3 \quad (12)$$

where t_3 represents the time after which fuel-N is consumed, i.e., $r_3 = 0$.

In fuel-rich flames, the reburning-NO mechanism becomes significant, with HCN recycling between NO and hydrocarbon radicals. Hence, a significant amount of HCN can be observed in the postflame region of fuel-rich flames (Figure 1). The reduction of NO by the reburning route can be added to eq 12, yielding the overall rate expression for HCN as follows:

$$-\frac{dX_{HCN}}{dt} = 2\frac{dX_{N_2}}{dt} + \left(\frac{dX_{NO}}{dt}\right)_{\text{fromHCN}} - \left(\frac{dX_{NO}}{dt}\right)_{\text{reburning}}, \quad t > t_2 \quad (13)$$

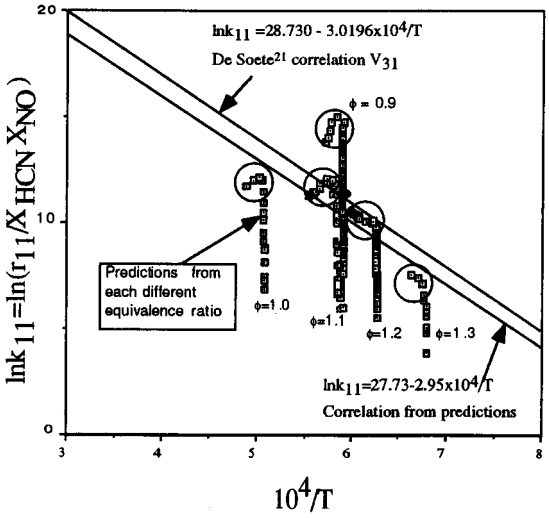

Simulation conditions:

ϕ	0.7 to 3.0
Fuel	C_2H_4
Oxidizer	O_2
Balance gases	Ar or He

Figure 9. Comparison of the rate constant derived from elementary kinetics with the experimentally deduced rate constant of De Soete.[21]

When NO is seeded into hydrocarbon flames, HCN is the dominant product from the reactions between NO and hydrocarbon radicals (Figure 3). The reduction steps of NO to HCN and then to N_2 are the rate-determining reactions in the NO reaction network. After the reduction of NO to a certain level, overall equilibrium among NO, HCN, and N_2 may be achieved, and an amount of residual HCN is expected.

Correlation of the Global Rate Parameters. The method used herein for determining k_8 and k_{11} from eqs 8, 11, and 12 was identical with that of De Soete[21] with one exception. De Soete determined mole fractions and their derivatives in the flow direction from test data, whereas in this study, the values were taken from calculated mole fraction profiles of one-dimensional, premixed flames. De Soete[21] evaluated the rate constants after fuel-N was mostly consumed. Similarly, in this work, fuel-N was considered as being mostly consumed when only 10% of the fuel-nitrogen compound (i.e., C_2N_2 or NH_3) remained. It is in this region that temperatures are sufficiently high to give realistic results.

Over 100 parametric simulations were completed for the various flames listed in Table 1 (with various values of ϕ, fuel-N, and fuel types). The computed profiles provided the necessary derivatives, which were more precise than the experimentally derived derivatives. Figure 9 illustrates a small number of the predicted k_{11} values vs temperature for five of the simulated flames. The numerical coefficients derived from the simulation for k_8 and k_{11} considered all the numerical values (more than a thousand points for each flame) through a curve fit of the log rate vs reciprocal temperature by the least-squares method. Most of these points overlapped each other and hence are represented by the large circles in Figure 9 for a given flame. Rate constant values vary substantially over a wide range of ϕ. However, almost all the k values occur at the higher levels, indicated by the large circles. The rate constants were not substan-

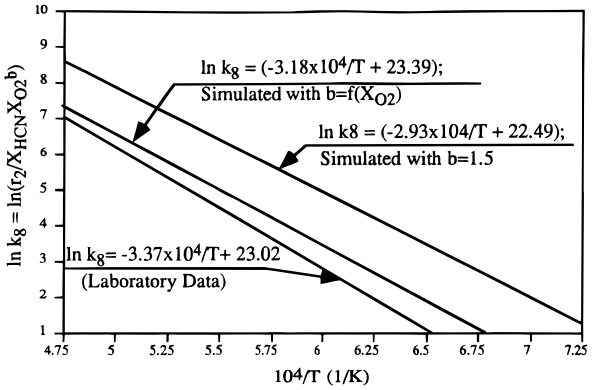

Figure 10. Comparisons between empirical and simulated correlations for k_8, where $r_8 = k_8 X_{HCN} X_{O_2}{}^b$. For the simulations $\phi = 0.7-1.0$. Conditions for the C_2H_4 flames are the same as those of De Soete.[21]

tially influenced by the few low values of k_{11} shown at lower temperatures in Figure 9.

The equation defined by De Soete[21] to correlate k_8 (without reburning and obtained by material balance of nitrogen atoms as shown in Figure 8) is

$$k_8 = \frac{-\frac{dX_{HCN}}{dt} + \frac{dX_{NO}}{dt} + V_D}{2X_{HCN}X_{O_2}{}^b} \qquad (14)$$

where V_D is the effect from the thermal-NO and b is the exponent for the oxygen concentration dependence.[21] The premixed flame simulations (e.g., Figures 5−7) provided required species profiles for deducing the global rates. However, in fuel-rich flames, the reburning-NO mechanism could be significant. Thus, the correlation of the global rate constants from the species profiles must include the effects of the reburning-NO mechanism.

The k_8 expression correlated from the simulations, shown in Figure 10, is

$$k_8 = 1.5 \times 10^{10} \exp\left(-\frac{63200}{RT}\right) \qquad (15)$$

This correlation was obtained from simulations at atmospheric pressure with C_2N_2 as fuel-N, helium as the inert gas in $C_2H_4-O_2$ flames, and an equivalence ratio range 0.7−1.0.

De Soete determined k_8 from experimental data to be

$$k_8 = 1 \times 10^{10} \exp\left(-\frac{67000}{RT}\right) \qquad (16)$$

where the units are kcal/mol, Kelvin, and mol/cm^3. This result is also illustrated in Figure 10. Previous modeling experience using eq 16 to predict NO_x formation in coal flames showed that the pre-exponential factor for eq 16 should be somewhat higher than De Soete's value.[37] This earlier work suggests a need to investigate these rate constants.

The values of k_8 in the correlation from the simulations are within 6% of those from correlation of measurements at higher flame temperatures (about 2100 K). The majority of data has been for fuel-rich flames,[21] and therefore, De Soete's empirical correlation may be lower because of the exclusion of the reburning-NO mechanism. At temperatures of about 1800 K, a typical coal−air flame temperature, the pre-exponential factor from the simulated correlation is about 5−12 times higher than that from the experimental correlation, which is more in keeping with the observations from Hill et al.[37] and Boardman and Smoot.[38]

At low flame temperatures (about 1600 K), the two rate constants differ somewhat (by about 17%), and the difference can result in quite different NO predictions. The experiences using the De Soete rate constants show that when a higher rate constant is used, the NO concentration in the near-burner region is much higher than observed, although downstream, NO is closer to the experimental measurement. When De Soete's lower rate constant is used, the near-burner NO concentration is much lower than measured.[38]

The correlation equation as defined by De Soete,[21] which comes from material balance of nitrogen atoms from global reactions 8 and 11, is

$$k_{11} = \frac{-\frac{dX_{HCN}}{dt} - \frac{dX_{NO}}{dt} - V_D}{2X_{HCN}X_{NO}} \qquad (17)$$

where V_D is the thermal-NO effect. The k_{11} value from the simulations is

$$k_{11} = 1.1 \times 10^{12} \exp\left(-\frac{58620}{RT}\right) \qquad (18)$$

while the experimental value reported by De Soete[21] is

$$k_{11} = 1.0 \times 10^{12} \exp\left(-\frac{60000}{RT}\right) \qquad (19)$$

The k_{11} values from simulated and experimental correlations are within 5% over the temperature range 1400−2100 K. The difference is within the error of the correlation, which is about 9%.[39] These two rate expressions were compared in Figure 9.

The above results demonstrate that reliable global rate parameters can be obtained directly from computations with comprehensive reaction mechanisms. This opens up the opportunity to apply this method to the deduction of the reaction rate for the $NO-CH_i$ reburning reaction:

$$CH_i + NO \rightarrow HCN + ... \qquad (20)$$

where no global rate (r_{20}) has been reported. The determination of r_{20} is the topic of a companion paper.9

The proposed global fuel-NO formation pathway illustrated by Figure 8 includes the reburning reaction 20. The global reburning-NO pathway is important when fuel-rich flames or NO-seeding flames are encountered. When fuel-N exists (>100 ppm), thermal-NO and prompt-NO may be negligible (<5%). HCN is also an

(37) Hill, S. C.; Smoot, L. D.; Smith, P. J. Predictions of nitrogen oxide formation in turbulent coal flames. *Twentieth Symposium (International) on Combustion*; The Combustion Institute: Pittsburgh, PA, 1984; p 1391.

(38) Boardman, R. D.; Smoot, L. D. Predictions of nitric oxide in advanced combustion systems. *AIChE J.* **1988**, *34*, 1573.

(39) Boardman, R. D. Further evaluation of a predictive model for nitric oxide formation during pulverized coal combustion. Master Thesis, Department of Chemical Engineering, Brigham Young University, Provo, Utah, 1987.

important intermediate species in the reduction of NO. The recycle in NO → HCN → N_2 or NO can be described by the global NO reaction mechanisms for fuel-NO and reburning. The global reburning-NO reaction should also be considered in fuel-rich flames with NH_3 as fuel-N. In other words, NO formed from NH_3 can also react with hydrocarbon radicals in fuel-rich flames and be reduced to HCN. The more complete NO formation pathway is illustrated in Figure 8.

Summary

Traditionally, experiments are used to identify rate-determining reactions and to determine global rate expressions by correlation of the measured species profiles. The experimental correlations of global rate constants may lead to errors because shifts in the rate-determining steps with the combustion conditions are not readily determined by such experiments. In addition, experiments are typically costly, difficult to perform accurately, and not readily amenable to required differentiation. Therefore, a less expensive and more general method for obtaining these global rate expressions is desirable.

By use of the methodology reported herein, two global rate expressions were obtained by generalized computations of premixed laminar flames using a comprehensive set of fundamental reaction rates. Premixed flames were simulated, and the major, intermediate, and radical species profiles in these flames were predicted. The dependence of species concentrations and rate constants of elementary steps on temperature and other species was calculated. This information was then used to conduct the sensitivity analysis to help identify the rate-determining steps. Two global rate expressions were identified from previous work and from these rate-determining reactions, and the rate constants were obtained through correlation based on the predicted species concentration profiles.

The reliability of the simulations and correlations depends on the completeness of the elementary chemical mechanisms used in the simulations and on the ranges of the dependent variables explored. The simulations reported herein show reasonably good agreement with premixed flame data. These results suggest that the elementary steps used provide reasonable fundamental rates and reactions of predictions under the simulated conditions, although comparisons in very fuel-rich and very fuel-lean regions were less reliable.

The sensitivity analyses of the premixed flame predictions suggested that reburning-NO elementary steps are significant when fuel-rich flames are encountered. Hence, the correlation of global fuel-N rate constants may lead to error without including the reburning-NO steps when fuel-rich flames are simulated. The comparisons of the global rates of NO formation and destruction also support the concept that the reburning-NO mechanism should be considered.

The rate constants determined from the competitive global reactions of HCN conversion to NO and to N_2 from simulations show good agreement with rates independently obtained by correlation of measured data. The rate constant (k_8) for the global reaction HCN + O_2 → NO + ... correlated from the predictions is within 16% of the k_8 constant experimentally obtained by De Soete[21] in the temperature range 1600−2100 K, while the value of k_{11} (NO + HCN → N_2 + ...) obtained here is within 5% of De Soete's reported value. This verifies both the full kinetic mechanism as being appropriate for simulating the experiments of De Soete and the methodology used to generate global rate constants from the full kinetic simulations. It may be possible to extend this technique to many other chemical reaction schemes, where appropriate rate-determining global steps have been identified. Care must be taken to express the limits of the conditions examined (i.e., temperatures, pressures, and equivalence ratios), since it is likely that such "global rate constants" change with conditions. The correlation of global rate constants from full kinetic mechanisms offers an alternative to reduced mechanisms where rate constants are functions of many elementary rate constants.

Acknowledgment. This research was sponsored by the Advanced Combustion Engineering Research Center. Funds for this Center are received from the National Science Foundation's Engineering Education and Centers Division, the State of Utah's Centers of Excellence, 36 industrial participants, and the U.S. Department of Energy. The authors appreciated technical suggestions and support from Dr. S. C. Hill and other colleagues during the research.

Glossary

CHEMKIN	CHEMical KINetic computer program
SENKIN	SENsitivity analysis of chemical KINetics program
b	exponent of oxygen concentrations in the data correlation of global reaction 8
CH_i	ith hydrocarbon species
C_i (g cm^{-3}; g mol cm^{-3})	concentrations of species i
k_j (gmol cm^{-3} s^{-1})	rate constant of reaction j
r_i (g mol cm^{-3} s^{-1})	global rate of the pathway i
R (cal g mol^{-1} K^{-1})	ideal gas constant
T (K)	temperature
S	sensitivity coefficient defined by eq 1
t (s or ms)	time
V_D (s^{-1})	thermal-NO effect in eq 14 and eq 17
X_i	mole fraction of species i in the gas phase
ϕ	equivalence ratio defined by the concentration of fuel divided by the concentration of oxygen

EF950169B